

STELLAR POPULATIONS OF THE DWARF GALAXY LGS 3 IN THE LOCAL GROUP¹

MYUNG GYOON LEE

Department of Astronomy, Seoul National University, Seoul 151-742, Korea
Electronic mail: mglee@astrog.snu.ac.kr

Received 1995 March 28

ABSTRACT

We present *VRI* CCD photometry of ~ 490 stars in the dwarf galaxy LGS 3 in the Local Group. The color–magnitude diagrams of LGS 3 show a well defined red giant branch (RGB), a small number of asymptotic giant branch stars, and several blue stars which are possibly young main-sequence stars. The tip of the RGB is found to be at $I_{\text{TRGB}}=20.6\pm 0.2$ mag and $(V-I)_{\text{TRGB}}=1.31\pm 0.05$ mag. From the I magnitude of the tip of the RGB, we estimate the distance modulus of LGS 3 to be $(m-M)_0=24.54\pm 0.21$ mag for an adopted extinction of $A_V=0.08$ mag, corresponding to a distance of 810 ± 80 kpc. This result shows that LGS 3 may be a satellite of M31 or M33 which are close to LGS 3 in the sky. We measure the mean color of the RGB at $M_I=-3.5$ mag (~ 0.5 mag fainter than the tip of the RGB) to be $(V-I)_{-3.5}=1.28\pm 0.05$ mag. From these values we estimate the mean metallicity of the RGB stars to be $[\text{Fe}/\text{H}]=-2.10\pm 0.22$ dex. The integrated magnitudes of LGS 3 within the aperture radius $r=106''$ are measured to be $V=14.26$ mag, $R=13.84$ mag, and $I=13.26$ mag. The absolute integrated magnitude of LGS 3 is derived to be $M_V=-10.35$ mag. The central surface brightness is measured to be $\mu_V(0)=24.81\pm 0.07$ mag arcsec⁻². Surface brightness profiles and star number density profiles based on star counts are well fitted by a King model with a core concentration parameter $c=\log(r_t/r_c)=1.25\pm 0.13$, where r_t and r_c represents the tidal radius and the core radius, respectively. The core radius is measured to be $r_c=49''\pm 3''$, corresponding to 190 ± 10 pc. The metallicity and the absolute magnitude of LGS 3 are consistent with the metallicity–luminosity relation for the dwarf spheroidal galaxies in the Local Group. © 1995 American Astronomical Society.

1. INTRODUCTION

LGS 3 is a low surface brightness galaxy which was discovered in the course of the search for faint, dwarf galaxies in the Local Group by Kowal *et al.* (1978). It is located about 12° southwest from M33, and 20° south of M31 in the sky. Kowal *et al.* resolved LGS 3 into stars in the deep IIIa-J Schmidt plate and suspected it to be a member of the Local Group.

Right after the discovery of LGS 3, Thuan & Martin (1979) detected H I emission from LGS 3 at a heliocentric velocity of -280 km s⁻¹, which is very similar to that of M31 ($v=-298$ km s⁻¹). Later Lo *et al.* (1993) found, from more detailed H I observations obtained using the VLA, that the H I distribution is roughly consistent with the stellar distribution and extends out to ~ 1 kpc. They estimated the H I mass of LGS 3 to be $2\times 10^5 M_\odot$ and the total mass of LGS 3 to be $1.8\pm 1\times 10^7 M_\odot$ using the virial theorem and velocity measurements, for an adopted distance to LGS 3 of 900 kpc. Then they derived a value for the mass-to-luminosity ratio of LGS 3, $M/L_B=26\pm 16 M_\odot/L_{B,\odot}$, which is much higher than that of typical dwarf irregular galaxies.

Schild (1980) estimated, from *R* band CCD photometry of LGS 3 obtained using the CCD camera with a large pixel

scale of $6''.15\times 4''.52$, that the *R* magnitude of the brightest stars is $R=18.3$ mag and that the total integrated magnitude within the aperture radius of $85''$ is $R=14.2$ mag. Christian & Tully (1983) presented *VR* CCD photometry of LGS 3, showing that LGS 3 begins to resolve into a rich population of red giants fainter than $V\approx 21.6$ mag. They suggested from the brightness of the brightest red giants they resolved that the distance to LGS 3 is $0.7\text{--}1.2$ Mpc, depending on whether these red stars belong to an intermediate age ($10^8\text{--}10^9$ yr) population or to an old population with age $>10^9$ yr. However, their photometry was not good enough for them to distinguish between these two possibilities.

Cook & Olszewski (1989) obtained *BVI* and *77–81* intermediate band photometry using the 4Shooter on the Palomar 5 m telescope. They discovered asymptotic giant branch carbon stars, and resolved the tip of the red giant branch at $V\approx 21.6$ mag and $(V-I)\approx 1.4$ mag. Also, they found little sign of a blue main sequence. However, the details are not yet published.

Tacconi & Young (1987) detected CO emission from LGS 3 at the heliocentric velocity of -310 km s⁻¹ in the search for CO in 15 dwarf irregular galaxies. They estimated the CO mass of LGS 3 to be $10^5 M_\odot$ for an adopted distance to LGS 3 of 820 kpc, showing that LGS 3 has the lowest CO luminosity ($L_{\text{CO}}=0.02$ K km s⁻¹ kpc⁻²) of any galaxies in which CO has been detected. Infrared luminosity from 1 to 500 μm of LGS 3 was estimated to be $<3.6\times 10^5 L_\odot$ (Young

¹Based in part on observations which were made with the Palomar 1.5 m telescope which is jointly operated by the California Institute of Technology and the Carnegie Institution of Washington.

TABLE 1. Journal of observations for LGS 3.

Filter	T(exp)	Air Mass	Seeing	UT(start)
<i>V</i>	3600 sec	1.47	1".3	1991 Dec 7 06:41
<i>R</i>	1800 sec	1.24	1".2	1991 Dec 7 06:06
<i>I</i>	1800 sec	1.83	1".4	1991 Dec 7 07:45

et al. 1989). No H_{α} emission was detected in LGS 3 (Hunter *et al.* 1993).

LGS 3 is a very unique galaxy, because it, as well as the Phoenix dwarf galaxy, has been considered to be in a transition stage from a dwarf irregular galaxy to a dwarf spheroidal galaxy (Cook & Olszewski 1989; van de Rydt *et al.* 1991). The study of the dwarf galaxies in the Local Group such as LGS 3 provides important clues for understanding the origin and evolution of the dwarf galaxies in general. The origin and evolution of the dwarf galaxies has been investigated several times, but it is still an open question [see the references in the recent review paper on the dwarf elliptical galaxies by Ferguson & Binggeli (1994)].

In this paper we present a study of the stellar populations of LGS 3 based on *VRI* CCD photometry. Section 2 describes observations and data reduction, and Sec. 3 illustrates color–magnitude diagrams. Sections 4 and 5 estimate the distance and metallicity, and Sec. 6 presents surface photometry and star counts. Section 7 discusses the characteristics of LGS 3 in relation with other dwarf galaxies in the Local Group. Finally the primary results are summarized in Sec. 8.

2. OBSERVATIONS AND DATA REDUCTION

2.1 Observations

VRI CCD images of the LGS 3 dwarf galaxy were obtained under photometric conditions on 1991 December 7 (UT) using the Tektronix 1024×1024 pixels CCD camera on the 1.5 m telescope of the Palomar Observatory. We rebinned the original CCD images with a 2×2 pixel² binning size. The resulting pixel scale of the CCD image is 0".756/pixel, giving a field size of 6'.35×6'.35. The journal of observations of LGS 3 is given in Table 1. Greyscale maps of *V* and *I* CCD images are shown in Fig. 1. The bright stars with $V < 22$ mag and the blue stars [$(V-I) < 0.5$ mag] are marked, respectively, by the squares and the circles in Fig. 1(a), and the bright asymptotic giant branch stars [$I < 21.6$ mag and $(V-I) > 1.0$ mag] are marked by the circles in Fig. 1(b).

We divided the area covered by the CCD images into three regions to distinguish the probable member stars of the galaxy from the field stars: the 2'.5×3'.3 galaxy field (G region), the intermediate field (I region) surrounding the galaxy field, and the control field (F region) which probably include few, if any, member stars. The center of the galaxy field is at the position ($X=200$ pix, $Y=270$ pix). The areas of the three fields are 8.25, 24.26, and 9.10 arcmin² (the corresponding area ratios are 0.91:2.66:1). The boundaries for each field are shown by the solid lines in Fig. 1.

2.2 Data Reduction

Instrumental magnitudes of stars in LGS 3 were obtained using the digital stellar photometry program DOPHOT (Schechter *et al.* 1993). The instrumental magnitudes were transformed onto the standard Johnson–Kron–Cousins system using the standards from Landolt (1983), Christian *et al.* (1985), and Davis (1990). The transformation equations are

$$V = v - 0.129X + 0.057(v - i) - 1.338,$$

$$(V - R) = 0.958(v - r) - 0.032X - 0.308, \quad \text{and}$$

$$I = i - 0.060X - 1.299,$$

where the lower case symbols represent instrumental magnitudes derived from the CCD images and the upper case symbols represent the standard system values. X is the airmass at the midpoint of the observations and the zero point for the instrumental magnitude was arbitrarily set to be 23.5 mag. The rms scatters of the standard stars were 0.04 mag for V , R , and I .

The total number of stars which were measured in our CCD field is ~ 490 . We listed the photometry of 87 bright stars with $V < 22$ mag in Table 2. The X and Y coordinates listed in Table 2 are given in units of CCD pixel. Mean photometric errors for the measured stars (formal errors from DOPHOT) are given in Table 3.

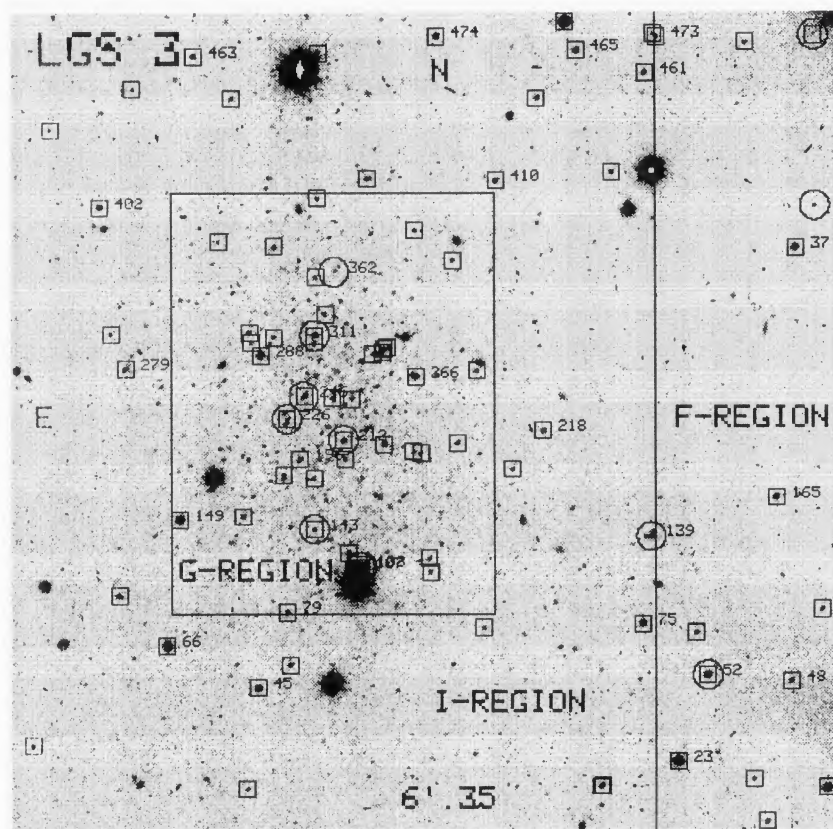
2.3 Comparisons with Previous Photometry

We have compared our photometry with the *VR* photometry given by Christian & Tully (1983). Figure 2 displays a comparison for 15 stars in common between ours and Christian & Tully's, which is also listed in Table 4. Figure 2 shows that our V magnitudes are systematically brighter than those by Christian & Tully and that our $(V-R)$ colors are slightly redder than those by Christian & Tully. The mean differences between our photometry and Christian & Tully's are $\Delta V = -0.27 \pm 0.29$ mag and $\Delta(V-R) = 0.03 \pm 0.20$, where Δ represents ours minus Christian & Tully's.

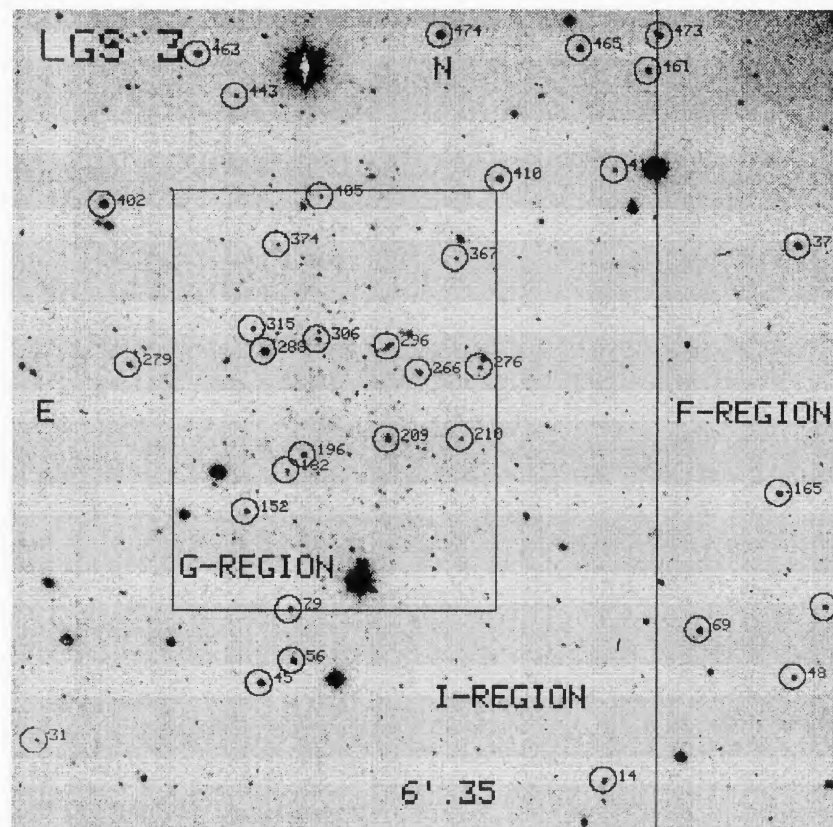
3. COLOR–MAGNITUDE DIAGRAMS OF LGS 3

We adopt in this study the foreground reddening value of $E(B-V) = 0.024$ mag for LGS 3 given by Burstein & Heiles (1984). The corresponding extinction values at V , R , and I are $A_V = 3.2E(B-V) = 0.08$ mag, $A_R = 0.07$ mag, and $A_I = 0.05$ mag. The internal reddening in LGS 3 is expected to be negligible, because there is no evidence of dark clouds and H II regions. We display $V-(V-I)$, $V-(V-R)$, $I-(V-I)$, and $I-(R-I)$ diagrams of ~ 490 measured stars in Fig. 3. The stars in the G region (245 stars), the I region (199 stars), and the F region (42 stars) are plotted by the filled circles, the open triangles, and the crosses, respectively. The contamination by the galactic foreground stars is estimated to be very low in the G region. Most of the resolved stars fainter than $V \approx 20$ mag in the G region are considered to be the members of LGS 3.

Several distinguishable features are seen in Fig. 3. First, there is a strong concentration of red stars fainter than



(a)



(b)

FIG. 1. (a) A V-band CCD image of LGS 3. North is at the top and east is to the left. The size of the frame is 6.35×6.35 . G region, I region, and F region represent the galaxy field, the intermediate field, and the control field, respectively. Bright stars with $V < 21$ mag (squares) and blue stars with $(V - I) < 0.5$ mag (circles) are labeled. The stars with $22 > V > 21$ mag are also marked by the squares. (b) An I-band CCD image of LGS 3. Bright asymptotic giant branch stars are labeled.

TABLE 2. Photometry of bright stars with $V < 22$ mag in LGS 3.

ID	X	Y	V	(V-R)	(V-I)	ID	X	Y	V	(V-R)	(V-I)
2	469.3	11.5	21.55	-0.20	0.88	246	181.5	275.0	21.59	0.22	0.01
10	146.4	32.0	21.95	0.64	1.41	266	250.8	287.3	19.37	0.56	1.11
11	506.1	32.5	17.91	0.53	0.95	276	288.7	290.7	21.52	0.84	1.62
13	366.0	33.5	21.86	—	1.89	279	71.5	291.8	20.05	0.75	1.50
14	366.8	34.4	21.44	—	1.25	288	154.8	300.2	18.92	0.96	2.08
16	460.8	38.1	21.91	0.45	0.74	289	224.4	300.7	21.95	0.66	1.26
23	413.7	49.3	17.49	0.79	—	292	229.5	302.5	21.88	0.57	1.20
31	14.9	58.5	21.42	0.33	1.02	296	231.4	303.5	21.59	0.61	1.55
45	152.9	94.9	19.40	0.92	1.97	299	233.2	304.6	21.94	0.47	1.32
48	484.0	99.4	20.88	0.86	1.85	306	188.1	307.5	21.44	1.02	1.94
52	432.2	102.8	19.43	0.11	0.37	307	149.0	307.7	21.99	0.65	1.41
56	173.1	109.2	21.52	1.42	3.41	308	162.5	311.4	21.89	0.76	1.23
66	97.3	120.7	17.80	0.52	0.98	311	188.4	312.4	20.08	0.02	-0.09
69	425.4	129.0	21.29	1.20	2.88	312	62.6	313.4	21.74	0.73	1.39
72	293.4	131.8	21.83	0.58	1.15	315	147.7	314.2	21.20	0.66	1.30
75	392.2	134.5	19.13	0.33	0.67	328	194.9	324.8	21.87	0.60	1.29
79	171.1	140.9	20.79	0.73	1.56	359	188.7	347.8	21.67	0.65	1.42
81	503.1	143.0	21.47	1.16	2.80	367	273.9	358.3	21.55	0.65	1.40
89	67.9	150.6	21.98	—	0.90	373	486.5	366.3	18.89	0.56	1.08
102	259.8	165.4	21.86	0.56	1.35	374	163.2	366.5	21.48	0.57	1.24
106	213.8	168.3	21.84	0.08	0.89	376	128.7	369.5	21.82	0.69	1.32
107	215.7	168.4	20.82	0.14	0.06	388	250.1	376.8	21.64	0.75	1.59
108	217.2	168.5	21.20	0.03	0.45	402	56.0	391.4	19.39	1.07	2.45
112	215.4	169.9	21.85	0.42	0.90	405	190.1	396.5	21.58	0.65	1.31
115	258.9	173.6	21.96	0.62	1.19	410	301.0	407.7	20.26	1.18	2.75
118	208.9	177.2	21.72	0.49	1.60	413	220.5	409.0	21.95	—	1.60
143	188.1	192.1	21.43	0.21	0.15	418	373.0	413.2	21.36	0.88	1.76
149	105.3	198.0	18.60	1.07	—	429	25.6	439.3	21.85	1.15	2.73
152	143.8	200.2	21.14	1.04	2.52	443	137.4	459.0	21.37	0.74	1.27
165	474.9	212.2	19.74	0.88	1.76	444	326.5	459.3	21.74	—	1.42
180	187.6	224.0	21.94	0.59	1.26	452	76.3	464.7	21.82	0.60	1.21
182	169.0	225.8	21.47	0.77	1.63	457	172.0	472.7	21.66	—	0.60
186	311.3	229.8	21.74	0.68	1.31	460	171.9	474.9	21.97	—	1.28
196	179.1	235.6	20.42	0.94	2.09	461	393.7	475.2	20.64	0.96	1.98
198	207.4	236.1	21.66	0.55	1.35	463	114.1	485.3	20.36	1.09	2.45
202	253.7	239.6	21.84	0.62	1.28	464	190.7	487.1	21.88	—	1.48
203	249.4	240.6	21.88	0.44	1.05	465	351.1	489.1	19.62	0.95	2.05
209	231.4	245.5	21.00	1.13	2.71	468	455.7	493.7	21.95	0.37	0.50
210	277.2	246.3	21.57	0.70	1.42	473	401.1	497.0	20.92	1.20	2.84
212	206.1	247.8	21.60	-0.22	0.19	474	264.4	497.5	19.36	1.05	2.37
218	330.3	253.7	20.64	0.31	0.59	475	498.0	498.3	21.96	-1.01	0.13
226	171.1	260.9	21.78	-1.01	-0.17	477	398.9	498.7	21.82	1.29	3.01
243	211.4	273.4	21.97	0.63	1.73	481	344.3	506.1	17.01	0.40	—
244	199.3	274.0	21.23	0.30	0.74						

$V \approx 21.4$ mag and $I \approx 19.8$ mag in the G region. Most of these stars are the giant branch stars. There is seen a gap around the level of $V \approx 21.7$ mag and $I \approx 20.4$ mag. The stars fainter than this gap are mostly the red giant branch (RGB) stars and a small number of stars brighter than this gap are the asymptotic giant branch (AGB) stars. The mean locus of the giant branch in the $I-(V-I)$ diagram is derived from the median colors of the RGB and is listed in Table 5. Thus, most of the resolved bright stars in LGS 3 are old red giants, as are the cases for the dwarf spheroidal galaxies in the Local

Group. This indicates that LGS 3 is closer to the dwarf spheroidal galaxy rather than to the dwarf irregular galaxy, although LGS 3 has been classified as a dwarf irregular galaxy.

Secondly, Fig. 3 shows that there are several blue stars with $(V-I) < 0.5$ mag [$(V-R) < 0.3$ mag]. The brightest among them is located at $V = 20.06$ mag and $(V-I) = -0.13$ mag and the rest of them are fainter than $V \approx 21.4$ mag. The positions of these stars in the CCD image are marked by the large circles in Fig. 1(a). Figure 1(a) shows that these blue

TABLE 3. Mean photometric errors for stars in LGS 3.

V	σ_V	$\sigma_{(V-R)}$	$\sigma_{(V-I)}$	I	σ_I	$\sigma_{(V-R)}$	$\sigma_{(V-I)}$
19.75	0.013	0.019	0.015	18.25	0.011	0.032	0.029
20.25	0.018	0.025	0.026	18.75	0.012	0.038	0.034
20.75	0.027	0.038	0.054	19.25	0.022	0.047	0.047
21.25	0.043	0.053	0.058	19.75	0.036	0.074	0.079
21.75	0.069	0.081	0.110	20.25	0.054	0.084	0.092
22.25	0.102	0.129	0.155	20.75	0.088	0.117	0.135
22.75	0.153	0.198	0.220	21.25	0.130	0.155	0.182
23.25	0.202	0.256	0.267	21.75	0.193	0.204	0.253

stars are concentrated in the G region. These blue stars are possibly young massive main-sequence stars, as discussed in Sec. 7.

4. DISTANCE

We estimate the distance to LGS 3 using the I magnitude of the tip of the RGB (called hereafter as TRGB), as described in Lee *et al.* (1993a). It was shown recently that the I magnitude of the TRGB is an excellent distance indicator for resolved galaxies with metal-poor populations ([Fe/H]

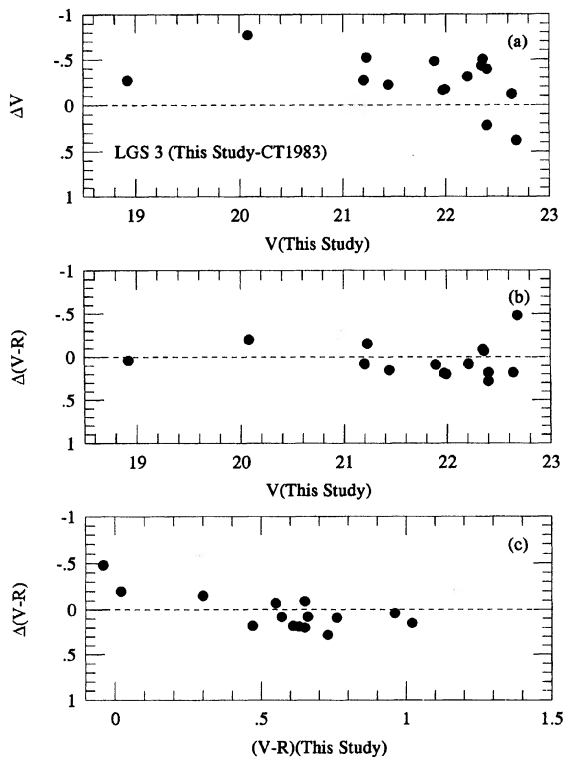


FIG. 2. Comparison of our photometry with Christian & Tully's (1983). Δ represents ours minus Christian & Tully's. (a) $\Delta V - V$ (this study) diagram. (b) $\Delta(V-R) - V$ (this study) diagram. (c) $\Delta(V-R) - (V-R)$ (this study) diagram.

TABLE 4. Comparison of our photometry with Christian & Tully's (1983).

This study					Christian & Tully (1983)			Difference	
ID	V	σ_V	$(V-R)$	$\sigma_{(V-R)}$	ID	V	$(V-R)$	$\Delta(V)$	$\Delta(V-R)$
228	22.35	0.09	0.65	0.10	6	22.78	0.74	-0.43	-0.09
230	22.40	0.15	0.61	0.16	49	22.79	0.43	-0.39	0.18
234	22.68	0.14	-0.04	0.21	61	22.30	0.44	0.38	-0.48
237	22.64	0.12	0.47	0.15	7	22.76	0.29	-0.12	0.18
243	21.97	0.07	0.63	0.09	4	22.12	0.44	-0.16	0.19
244	21.23	0.04	0.30	0.06	37	21.75	0.45	-0.52	-0.15
249	22.36	0.09	0.55	0.11	35	22.86	0.62	-0.50	-0.07
288	18.92	0.01	0.96	0.02	1	19.19	0.92	-0.27	0.04
306	21.44	0.04	1.02	0.05	3	21.66	0.87	-0.22	0.15
307	21.99	0.08	0.65	0.09	5	22.16	0.45	-0.17	0.20
308	21.89	0.07	0.76	0.08	10	22.37	0.67	-0.48	0.09
311	20.08	0.02	0.02	0.03	2	20.85	0.22	-0.77	-0.20
315	21.20	0.04	0.66	0.05	31	21.47	0.58	-0.27	0.08
323	22.40	0.12	0.73	0.14	57	22.18	0.45	0.22	0.28
342	22.21	0.09	0.57	0.12	42	22.52	0.49	-0.31	0.08

< -0.7 dex) older than a few Gyr, with an accuracy comparable to that of RR Lyraes and Cepheids (Lee 1993; Lee *et al.* 1993a).

The I magnitude of the TRGB is estimated using the $I - (V - I)$ diagram and the luminosity functions of red stars. Figure 4 shows the V and I luminosity functions of the measured stars in the G region and the I region which are listed in Table 6. In Fig. 4, as the magnitude increases, there is a sudden increase at $I = 20.6 \pm 0.2$ mag and $V = 21.9 \pm 0.2$ mag, which corresponds to the TRGB. The median value for the color of the TRGB is estimated to $(V - I)_{\text{TRGB}} = 1.31 \pm 0.05$ mag for 12 RGB stars with $20.5 < I < 20.7$ mag. The bolometric magnitude of the TRGB is then calculated from $M_{\text{bol}} = -0.19[\text{Fe}/\text{H}] - 3.81$ (Da Costa & Armandroff 1990). Adopting a mean metallicity of $[\text{Fe}/\text{H}] = -2.10 \pm 0.22$ dex as estimated in the next section, we obtain a value for the bolometric magnitude of $M_{\text{bol}} = -3.41$ mag. The bolometric correction at I for the TRGB is estimated to be $\text{BC}_I = 0.57$ mag, adopting a formula for the bolometric correction $\text{BC}_I = 0.881 - 0.243(V - I)_{\text{TRGB}}$ (Da Costa & Armandroff 1990). The intrinsic I magnitude of the TRGB is then given by $M_I = M_{\text{bol}} - \text{BC}_I = -3.98$ mag. Finally, the distance modulus of LGS 3 is obtained: $(m - M)_0 = 24.54 \pm 0.21$ mag (corresponding to a distance of 810 ± 80 kpc) for an adopted extinction of $A_V = 0.08$ mag, confirming that LGS 3 is a member of the Local Group.

A previous estimate for the distance to LGS 3 was given by Christian & Tully (1983), who obtained VR CCD photometry of bright stars in LGS 3. They suggested from the brightness of the brightest red stars in LGS 3 that the distance to LGS 3 is 0.7–1.2 Mpc, depending on whether these red stars belong to an intermediate age (10^8 – 10^9 yr) population or to an old population with age 10^9 yr. Our estimate is consistent with theirs, but the error in our estimate is much smaller than theirs.

5. METALLICITY

We have estimated the mean metallicity of the RGB stars in LGS 3 using the $(V - I)$ colors at $M_I = -3.5$ mag (~ 0.5

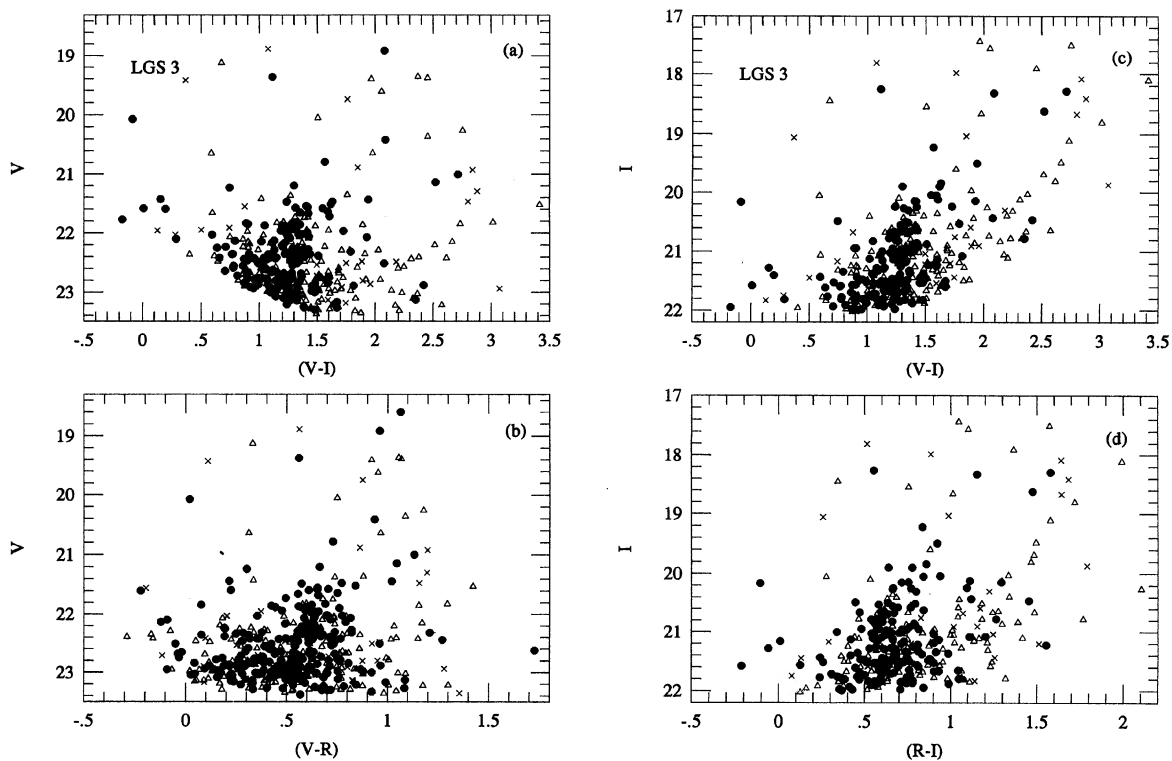


FIG. 3. Color-magnitude diagrams for all the measured stars in the CCD images of LGS 3. The stars in the G region, the I region, and the F region are plotted, respectively, by the filled circles, the open triangles, and the crosses. (a) $V-(V-I)$ diagram. (b) $V-(V-R)$ diagram. (c) $I-(V-I)$ diagram. (d) $I-(R-I)$ diagram.

mag fainter than the TRGB) (Da Costa & Armandroff 1990; Lee *et al.* 1993a). We measure the mean color of the 29 red stars with $20.9 < I < 21.2$ mag and $0.7 < (V-I) < 1.7$ mag to be $(V-I)_{-3.5} = 1.28 \pm 0.05$ mag. Using the calibration based on the RGB colors of galactic globular clusters (Da Costa & Armandroff 1990; Lee *et al.* 1993a), we obtain a value for the mean metallicity of $[\text{Fe}/\text{H}] = -2.10 \pm 0.22$ dex.

In Fig. 5, the RGB of LGS 3 is compared with the RGBs of the galactic globular clusters M15, M2, and NGC 1851, the metallicities of which are $[\text{Fe}/\text{H}] = -2.17$, -1.58 , and -1.29 dex, respectively. The RGBs of the galactic globular clusters were shifted vertically and horizontally according to the reddening and distance of LGS 3. Figure 5 shows that the mean RGB of LGS 3 is reasonably well fit by the mean RGB of M15. The mean photometric errors of the measured stars in LGS 3 are plotted by the error bars. The spread in the

colors of the measured stars in LGS 3 is consistent with the photometric errors.

The bright red stars above the tip of the RGB are mostly AGB stars. We compare the AGB population of LGS 3 with that of the Leo I dwarf spheroidal galaxy in Fig. 6. Leo I has a rich population of AGB stars of intermediate age (2–10 Gyr). The metallicity of Leo I is $[\text{Fe}/\text{H}] = -2.0$ dex, very similar to that of LGS 3. The total absolute magnitude of Leo I is $M_V = -12$ mag, which is 1.65 mag brighter than LGS 3 (Lee *et al.* 1993b; Demers & Irwin 1993). Figure 6 displays $M_I-(V-I)$ diagrams of LGS 3 and Leo I (Lee *et al.* 1993b) in the same scale. Figure 6 shows that the distribution of the AGB population of LGS 3 in the color-magnitude diagram is similar to the faint AGB stars of Leo I and that the brightest AGB stars in LGS 3 are ~ 0.4 mag fainter than those in Leo I.

TABLE 5. Mean $I-(V-I)$ locus for the giant branch of LGS 3.

I	$(V-I)$
19.75	1.62
20.25	1.41
20.75	1.29
21.25	1.28
21.75	1.12

6. SURFACE PHOTOMETRY AND STAR COUNTS

6.1 Surface Photometry

The shape of LGS 3 seen in the CCD images of Fig. 1 is elliptical, rather than irregular. The ellipticity and position angle of LGS 3 are estimated roughly to be $\epsilon \approx 0.2$ and $\text{PA} \approx 0^\circ$. Integrated and differential surface photometry of LGS 3 have been obtained using elliptical apertures with the ellipticity of $\epsilon = 0.2$ and the position angle of 0° . The photometry has been obtained following the method outlined by Djorgovski (1988) and Lee (1990). The elliptical annulus

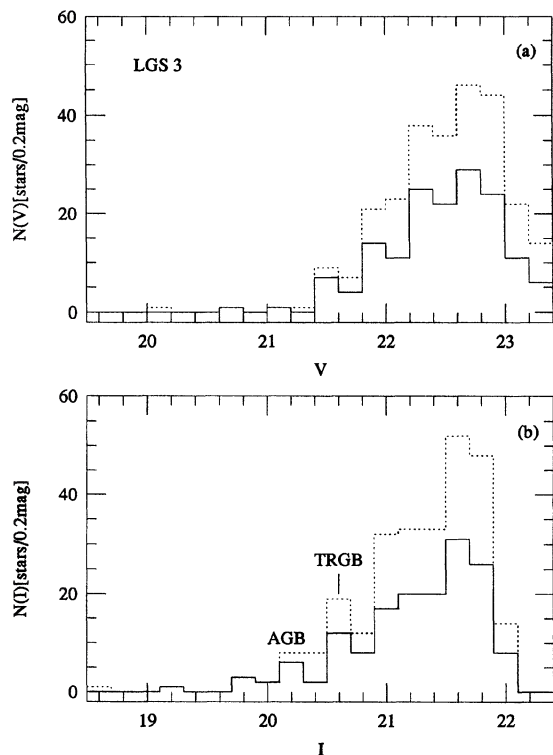


FIG. 4. Luminosity functions for the red stars in LGS 3. The solid lines and dotted lines represent the G region, and the sum of the G region and I region, respectively. The positions of the TRGB and the AGB are labeled. (a) V luminosity function. (b) I luminosity function.

apertures were divided into eight azimuthal sectors. The error of the differential surface photometry is determined from the standard error of the mean value for the eight sectors. Before performing the surface photometry we removed from

TABLE 6. I and V luminosity functions for LGS 3.

I	$N(I)$		V	$N(V)$	
	G-region	I-region		G-region	I-region
19.8	3	0	21.1	1	0
20.0	2	0	21.3	0	1
20.2	6	2	21.5	7	2
20.4	2	6	21.7	4	3
20.6	12	7	21.9	14	7
20.8	8	4	22.1	11	12
21.0	17	15	22.3	25	13
21.2	20	13	22.5	22	14
21.4	20	13	22.7	29	17
21.6	31	21	22.9	24	20
21.8	26	22	23.1	11	11

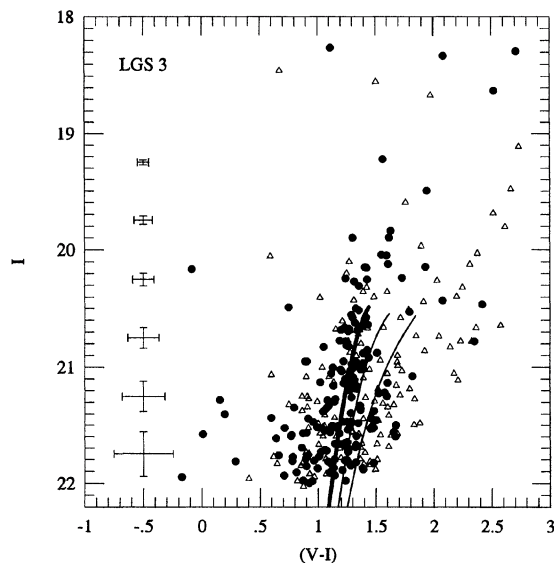


FIG. 5. $I-(V-I)$ diagram for stars in LGS 3 in comparison with galactic globular clusters. The solid curved lines show, from left to right, the loci for the giant branches of galactic globular clusters, M15, M2, and NGC 1851, the metallicities of which are $[Fe/H] = -2.17, -1.58,$ and -1.29 dex, respectively. The mean errors for the magnitudes and colors are illustrated by the error bars.

the CCD images the bright stars which are judged to be the foreground stars based on the color-magnitude diagrams. Table 7 lists the integrated and differential surface photometry of LGS 3. The radii (r) are given in terms of a geometrical mean of the major and minor axes of the ellipse (a and b): $r = \sqrt{ab}$.

The distributions of integrated light and color as well as surface brightness and color profiles are plotted in Fig. 7, as listed in Table 7. The integrated magnitudes within the aperture radius of $106''$ are measured to be $V = 14.26 \pm 0.04$ mag,

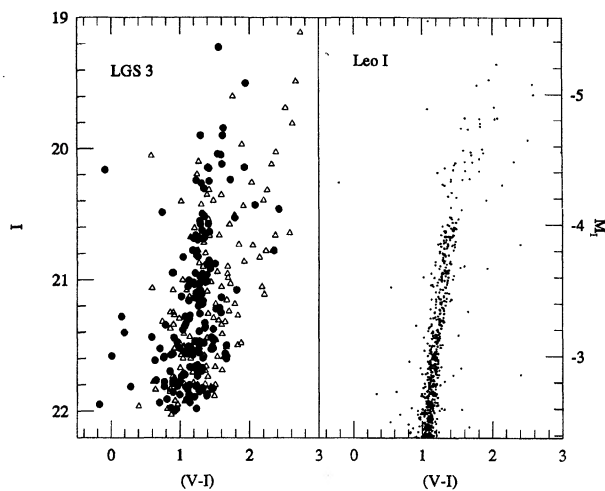


FIG. 6. Comparison of the $M_I-(V-I)$ diagrams for LGS 3 and the Leo I dwarf spheroidal galaxy given by Lee *et al.* (1993b). Both are plotted in the same scale and the diagram for Leo I was shifted according to the distance to LGS 3. Note the similarity of the distribution of AGB stars in both galaxies.

TABLE 7. Surface photometry of LGS 3.

$r_{\text{eff}}['']$	$r_{\text{out}}['']$	$\mu_V(r)$	$\mu_R(r)$	$\mu_I(r)$	V	R	I
4.7	6.7	24.81 ± 0.07	24.45 ± 0.07	24.26 ± 0.07	19.46	19.08	18.88
8.9	10.6	24.95 ± 0.04	24.59 ± 0.03	24.50 ± 0.06	18.42	18.05	17.92
14.1	16.8	24.91 ± 0.03	24.56 ± 0.03	24.36 ± 0.03	17.39	17.03	16.85
22.3	26.7	25.08 ± 0.01	24.76 ± 0.02	24.50 ± 0.03	16.47	16.14	15.91
35.4	42.3	25.26 ± 0.03	24.84 ± 0.04	24.34 ± 0.07	15.62	15.24	14.84
56.1	67.1	25.64 ± 0.06	25.28 ± 0.05	24.74 ± 0.07	14.88	14.51	14.04
78.7	88.8	26.00 ± 0.08	25.56 ± 0.06	24.93 ± 0.06	14.47	14.09	13.55
98.0	106.3	26.37 ± 0.09	25.89 ± 0.08	25.10 ± 0.07	14.26	13.84	13.26

$R=13.84 \pm 0.04$ mag, and $I=13.26 \pm 0.04$ mag. From these values we derive the absolute integrated magnitudes of $M_V=-10.35$ mag, $M_R=-10.76$ mag, and $M_I=-11.32$ mag. The central surface brightnesses are measured to be $\mu_V(0)=24.81 \pm 0.07$ mag, $\mu_R(0)=24.45 \pm 0.07$ mag, and $\mu_I(0)=24.26 \pm 0.07$ mag. Figure 7(d) shows that the $(V-R)$ colors get slightly redder as the radius increases, and that the $(V-I)$ colors get significantly redder with the increasing radius. However, better VI photometry is needed to check our VI colors for the outer area of LGS 3, because the sky background in the I image is so high that a reliable photometry of the outer part of LGS 3 is difficult to be derived from our data.

6.2 Star Counts

Since the surface brightness in the outer area of LGS 3 is too low to be measured reliably, we have counted stars to

TABLE 8. Star number density of LGS 3.

$r_{\text{eff}}['']$	$r_{\text{out}}['']$	N	$N[\text{stars arcsec}^{-2}]$
10.6	15.0	13	0.0183 ± 0.0051
18.3	21.1	10	0.0147 ± 0.0046
26.0	30.1	17	0.0117 ± 0.0028
37.0	42.9	25	0.0085 ± 0.0017
52.2	60.2	42	0.0075 ± 0.0012
73.6	85.0	53	0.0047 ± 0.0006
104.2	120.3	54	0.0024 ± 0.0003
134.1	146.6	30	0.0014 ± 0.0003
160.3	173.0	30	0.0013 ± 0.0002

derive the number density distribution of the outer area of LGS 3, supplementing the surface photometry. Table 8 lists the star counts of LGS 3.

We have combined the V surface brightness profiles with the number density profiles based on the star counts in Fig. 8. We fit the resulting profiles with the single-mass isotropic King models (King 1966). Figure 8 shows that the surface brightness profiles combined with the number density profiles are well fitted by a King model with a core concentra-

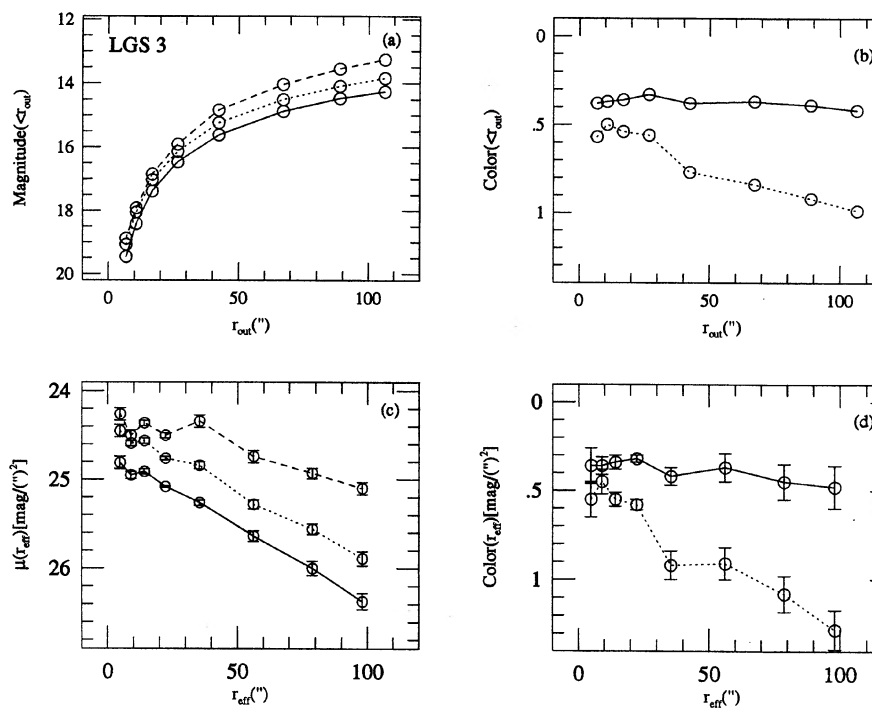


FIG. 7. Surface photometry of LGS 3. The radii are given in terms of $r = \sqrt{ab}$ where a and b represent, respectively, the major and minor axes of the ellipse. r_{out} represents the outer radius of the given aperture and r_{eff} represents the effective radius of the given annular aperture. (a) Integrated magnitudes vs r_{out} . V , R , and I magnitudes are represented by the solid line, the dotted line, and the dashed line, respectively. (b) Integrated colors vs r_{out} . $(V-R)$ colors and $(V-I)$ colors are represented by the solid line and the dotted line, respectively. (c) Surface brightness profiles vs effective radius. V , R , and I magnitudes are represented by the solid line, the dotted line, and the dashed line, respectively. (d) Differential colors vs effective radius. $(V-R)$ colors and $(V-I)$ colors are represented by the solid line and the dotted line, respectively.

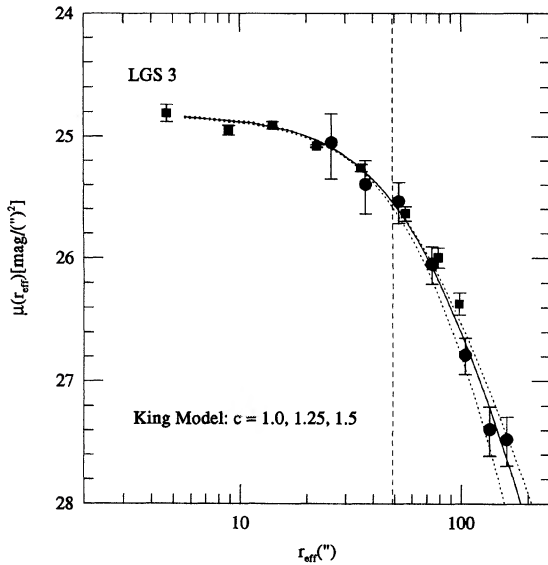


FIG. 8. Surface brightness profiles combined with star number density profiles of LGS 3 and an adopted King model fit. The squares represent the V surface brightness profiles and the circles represent the star number density profiles based on star counts. The star number density profiles were arbitrarily shifted vertically to match the surface brightness profiles. The dotted and solid curved lines represent, from left to right, the single-mass isotropic King models with core concentration parameters of $c=1.0$, 1.25 , and 1.50 , respectively.

tion parameter $c = \log(r_t/r_c) = 1.25 \pm 0.13$. The core radius is measured to be $r_c = 49'' \pm 3''$, corresponding to 190 ± 10 pc.

7. DISCUSSION

7.1 Is LGS 3 a Satellite Galaxy of M31 or M33?

To date there are seven known satellite dwarf galaxies of M31:M32, NGC 205, NGC 185, NGC 147, And I, And II, and And III. LGS 3 has also been suspected to be a satellite galaxy of M31 or M33, because LGS 3 is located 12° from M33 and 20° from M31 in the sky. We inspect this possibility using the distance estimate of LGS 3 we obtained in this study.

The distances to M31 and M33 based on the same TRGB method as applied to LGS 3 are 770 kpc and 870 kpc, respectively (Mould & Kristian 1986; Lee *et al.* 1993a). Therefore, LGS 3 is located at the distance of 274 kpc from M31, and 174 kpc from M33 (the distance between M31 and M33 is 233 kpc). The distance between M31 and LGS 3 is very similar to that between the Milky Way Galaxy and Leo I, which is the most distant known satellite galaxy of the Milky Way Galaxy, 270 kpc (Lee *et al.* 1993b). In addition, the systemic velocities of LGS 3, M31, and M33 with respect to the center of the Local Group are -59 , -26 , and 48 km s $^{-1}$, respectively (Schmidt & Boller 1992). These results lead us to conclude that LGS 3 is probably a satellite galaxy of M31 and/or M33.

7.2 The Metallicity and Luminosity Relation of Dwarf Galaxies

The metallicity and luminosity relation in dwarf spheroidals and dwarf ellipticals provides a critical clue for investigating the origin of dwarf galaxies. For this reason it has been studied several times, but the strengths of its correlation is controversial [see the references in Caldwell *et al.* (1992) and Lee *et al.* (1993b)]. In this section we compare the metallicity and luminosity of LGS 3 and those of other dwarf galaxies. We use the data compiled by Lee *et al.* (1993b) which are updated in this study. The absolute integrated magnitude of the Fornax dSph was reestimated to be $M_V = -13.1$ mag recently by Demers *et al.* (1994). The absolute integrated magnitude of the Sextans dSph is based on the mean of the estimates by Caldwell *et al.* (1992) and Irwin & Hatzidimitriou (1993): $M_V = -9.5$ mag (Hargreaves *et al.* 1994). The metallicity, the integrated magnitude, and the central surface brightness for the newly found Sag dSph are from Ibata *et al.* (1994) and Mateo *et al.* (1994): $[\text{Fe}/\text{H}] = -1.2$ dex, $M_V \approx -13$ mag, and $\mu_V(0) = 25.4$ mag. The metallicity for the Carina dSph is taken from Smecker-Hane *et al.* (1994): $[\text{Fe}/\text{H}] = -2.2$ dex. The metallicity for And II is taken from König *et al.* (1993): $[\text{Fe}/\text{H}] = -1.59$ dex. The metallicity for the Leo II is taken from Lee (1995): $[\text{Fe}/\text{H}] = -1.93$ dex. We also add the nearby dwarf irregulars for comparison: SMC, IC 1613, NGC 6822, WLM, and NGC 3109 (Lee *et al.* 1993a).

The metallicities for LGS 3 and all dwarf ellipticals and spheroidals are plotted against the absolute V magnitude in Fig. 9(a) and against the V central surface brightness in Fig. 9(b), as are listed in Table 9. The dwarf irregulars are also plotted by the crosses in Fig. 9(a). The solid lines represent the linear least-square fit to the data for the dwarf ellipticals and spheroidals excluding the Sag, And I, Leo I dSphs: $[\text{Fe}/\text{H}] = -0.16(\pm 0.01)M_V - 3.51(\pm 0.15)$ with a standard deviation of $\sigma[\text{Fe}/\text{H}] = 0.10$ dex, and $[\text{Fe}/\text{H}] = -0.24(\pm 0.02)\mu_V(0) + 3.86(\pm 0.55)$ with a standard deviation of $\sigma[\text{Fe}/\text{H}] = 0.12$ dex. LGS 3 and Phoenix are located among the dwarf spheroidals, following the relations defined by the dwarf ellipticals and spheroidals. This comparison shows that these two galaxies are close to the stage of the dwarf spheroidals.

7.3 The Class of LGS 3

Dwarf galaxies refer generally to faint galaxies with the absolute magnitude of $M_B > -16$ mag. There are several kinds of dwarf galaxies: dwarf ellipticals, dwarf irregulars, dwarf spirals, blue compact dwarfs, and dwarf spheroidals [see Gallagher & Wyse (1994) and Ferguson & Binggeli (1994) for more details]. Among these we describe briefly only dwarf spheroidals and dwarf irregulars, because they are related with the classification of LGS 3. Dwarf spheroidals are the faintest of the dwarf galaxies and are loosely defined in this study as dwarf galaxies with the absolute magnitude of $M_V > -14$ mag and the central surface brightness of $\mu_V(0) > 22$ mag arcsec $^{-2}$. These criteria are based on

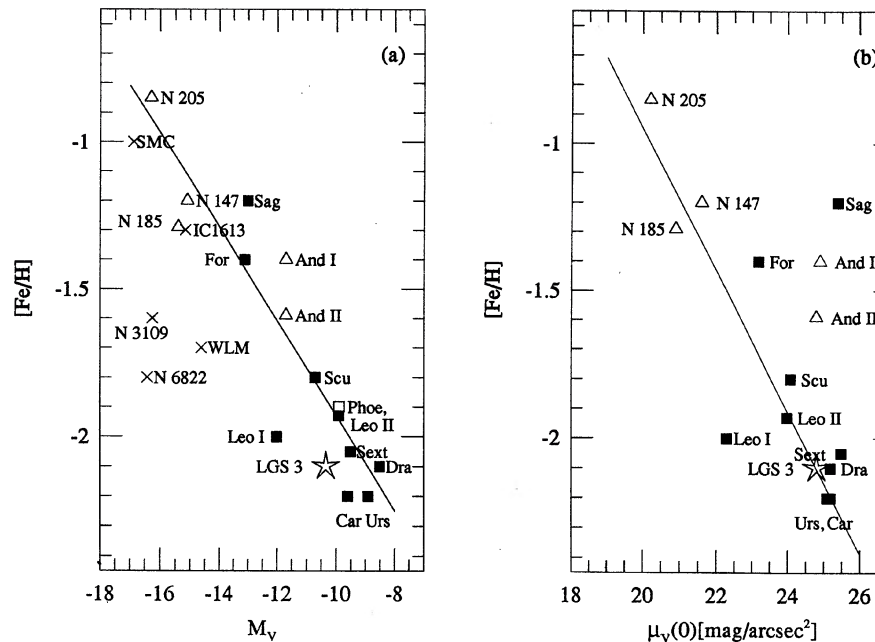


FIG. 9. (a) $[\text{Fe}/\text{H}]$ vs M_V for nearby dwarf elliptical, spheroidal, and irregular galaxies. The filled squares represent the satellite dwarf spheroidal galaxies of the Milky Way Galaxy, the open triangles represent the satellite galaxies of M31, and the crosses represent the dwarf irregular galaxies. LGS 3 is plotted by a star mark and Phoenix is marked by the open square. The solid line represents a linear fit for all the dwarf elliptical and spheroidal galaxies excluding the Sagittarius dSph, Andromeda I, Leo I, and LGS 3. (b) $[\text{Fe}/\text{H}]$ vs V central surface brightness. The solid line represents a linear fit for all the dwarf elliptical and spheroidal galaxies excluding the Sagittarius dSph, Andromeda I, Leo I, and LGS 3. Note that LGS 3 is located among the dwarf spheroidal galaxies.

the separation between the faintest of the historically known as dwarf ellipticals in the Local Group (NGC 147 and NGC 185) and the brightest of the historically known as dwarf spheroidals in the Local Group (Fornax and Leo I), as seen in Fig. 9. Dwarf irregulars usually refer to dwarf galaxies which are mostly a few or more magnitudes brighter than dwarf spheroidals and are gas-rich, showing a significant evidence of recent star formation.

LGS 3 was classified as a dwarf irregular galaxy right after its discovery. However, it was considered later to be in the transition stage between the dwarf irregular and the dwarf spheroidal galaxy by Cook & Olszewski (1989). The Phoenix dwarf galaxy is also known to be intermediate between the dwarf irregulars and the dwarf spheroidals and has H I gas of $\mathcal{M}(\text{H I}) = 10^5 \mathcal{M}_\odot$ (van der Rydt *et al.* 1991; Carignan *et al.* 1991). LGS 3 shows several features showing that it is closer to the dwarf spheroidals rather than to the dwarf irregulars: (1) the absolute magnitude of LGS 3 is $M_V = -10.35$ mag. LGS 3 is ~ 4 mag fainter than the faintest known dwarf irregular galaxy in the Local Group, WLM, which has an absolute magnitude of $M_V = -14.62$ mag (Lee *et al.* 1993a). (2) The structural shape of LGS 3 is elliptical, not irregular. The ellipticity of LGS 3 is approximately 0.2. (3) The surface brightness profiles and the star density profiles are well fitted by a King model. (4) The dominant population of the bright resolved stars is red giants. There are only a few blue stars which are possibly young main-sequence stars. (5) The metallicity and luminosity of LGS 3 are consistent with the $[\text{Fe}/\text{H}] - M_V$ relation of the dwarf spheroidal galaxies. (6) There is no H α emission detected in LGS 3,

showing that there is no sign of recent star formation (Hunter *et al.* 1993).

The only evidence indicating a dwarf irregular type is the presence of the H I gas ($2 \times 10^5 \mathcal{M}_\odot$) and CO gas ($1 \times 10^5 \mathcal{M}_\odot$) (Lo *et al.* 1993; Tacconi & Young 1987). Most of dwarf spheroidals have very little gas. The estimated masses of the H I gas in the dwarf spheroidals are: $< 10^3 \mathcal{M}_\odot$ for Carina (Mould *et al.* 1990); $< 10^4 \mathcal{M}_\odot$ for Fornax, Leo I, and Leo II; $280 \mathcal{M}_\odot$ for Ursa Minor; $68 \mathcal{M}_\odot$ for Draco (Knapp *et al.* 1978); and $51 - 75 \mathcal{M}_\odot$ for the Sag dSph (Koribalski *et al.* 1994). However, Sculptor may contain H I gas of $10^5 \mathcal{M}_\odot$ (Knapp *et al.* 1978), which is similar to that of Phoenix, $10^5 \mathcal{M}_\odot$ (Carignan *et al.* 1991). Thus, LGS 3, Phoenix, and Sculptor have relatively more H I gas than other dwarf spheroidals. However, the H I masses in these galaxies are more than an order of magnitude less than those in the faintest known dwarf irregulars in the vicinity of the boundary of the Local Group such as DDO 155 (=GR8) and DDO 210 (Lo *et al.* 1993). The H I masses in DDO 155 and DDO 210 are $2 \times 10^6 \mathcal{M}_\odot$ and $2 \times 10^6 \mathcal{M}_\odot$, respectively. The absolute magnitudes of DDO 155 and DDO 210 are, respectively, $M_B = -10.5$ mag and $M_B = -9.9$ mag. Therefore, the H I masses in LGS 3 and Phoenix are intermediate between those in the dwarf irregulars and the dwarf spheroidals. We suggest, considering the results described above, to classify the low surface brightness dwarf galaxies as dwarf spheroidals if they satisfy the following conditions: (1) the absolute magnitude is larger than $M_V = -14$ mag; (2) the morphological structure is not irregular; (3) the amount of the H I gas is less than $10^6 \mathcal{M}_\odot$; (4) the central surface brightness is fainter

TABLE 9. Luminosity, metallicity, and central surface brightness of nearby dwarf galaxies.

Galaxy	Type	M_V	[Fe/H]	$\mu_V(0)$ [mag arcsec $^{-2}$]
Draco	dSph	-8.5	-2.1	25.2
Ursa Minor	dSph	-8.9	-2.2	25.1
Sextans	dSph	-9.5	-2.05	25.5
Carina	dSph	-9.6	-2.2	25.2
Leo II	dSph	-9.9	-1.93	24.0
Phoenix	dSph/dIrr	-9.9	-1.90	—
Sculptor	dSph	-10.7	-1.80	24.1
Leo I	dSph	-12.0	-2.0	22.3
Sagittarius	dSph	-13.0	-1.2	25.4
Fornax	dSph	-13.1	-1.40	23.2
LGS 3	dSph/dIrr	-10.4	-2.10	24.8
And III	dSph	-10.2	—	25.3
And I	dSph	-11.7	-1.40	24.9
And II	dSph	-11.7	-1.59	24.8
NGC 147	dE	-15.1	-1.20	21.6
NGC 185	dE	-15.4	-1.29	20.9
NGC 205	dE	-16.3	-0.85	20.2
WLM	dIrr	-14.6	-1.6	—
IC1613	dIrr	-15.2	-1.3	—
NGC 6822	dIrr	-16.4	-1.8	—
NGC 3109	dIrr/dSp	-16.3	-1.6	—
SMC	dIrr	-16.9	-1.0	—

than $\mu_V(0)=22$ mag arcsec $^{-2}$. According to these criteria, LGS 3 and Phoenix are classified as dwarf spheroidals.

7.4 Blue Stars in LGS 3

Several blue stars of LGS 3 are seen in the color-magnitude diagrams (Fig. 3). We have found that the upper boundary of these blue stars extends up to $M_V \approx -3.0$ mag, and that the single brightest star has an absolute magnitude of $M_V \approx -4.5$ mag, adopting the distance estimate in this study. The distribution of these stars in the color-magnitude diagram is similar to that of the blue stars in the Phoenix dwarf galaxy (van de Rydt *et al.* 1991). The blue stars in Phoenix are mostly extending up to $M_V \approx -3.0$ mag (the single brightest one has an absolute magnitude of $M_V \approx -4.0$ mag). Thus, the blue stars seen in LGS 3 are possibly young massive main-sequence stars. Deeper photometry is needed to study in detail the main sequence of LGS 3.

8. SUMMARY AND CONCLUSIONS

We have presented a study of the stellar populations in the LGS 3 dwarf galaxy in the Local Group based on *VRI* CCD photometry. The primary results obtained in this study are

TABLE 10. Basic information for LGS 3.

Parameter	Information	Reference
$\alpha_{1950}, \delta_{1950}$	01 ^h 01 ^m 12 ^s , +21°38'	1
l, b	126.75 deg, -40.90 deg	1
HI heliocentric radial velocity, v_{\odot}	-277 km s $^{-1}$	1
Foreground reddening, $E(B - V)$	0.024 mag	2
V central surface brightness, $\mu_V(0)$	24.81 \pm 0.07 mag arcsec $^{-2}$	3
$V(r < 106'')$	14.26 \pm 0.04 mag	3
$(V - R)(r < 106'')$	0.42 \pm 0.04 mag	3
M_V	-10.35 mag	3
Metallicity, [Fe/H]	-2.10 \pm 0.22 dex	3
Distance modulus, $(m - M)_0$	24.54 \pm 0.21 mag	3
Distance	810 \pm 80 kpc	3
Core radius	49'' \pm 3'' (190 \pm 10 pc)	3
Ellipticity	\sim 0.2	3
Position angle	\sim 0 deg	3
$M(\text{HI})$	$2 \times 10^5 M_{\odot}$	1,3
$M(\text{CO})$	$1 \times 10^5 M_{\odot}$	4
Total mass	$2 \times 10^7 M_{\odot}$	1,3
Mass-luminosity ratio, M/L_V	16 $M_{\odot}/L_{V,\odot}$	1,3

References—(1) Lo *et al.* (1993); (2) Burstein & Heiles (1984); (3) This study; (4) Tacconi & Young (1987).

summarized as follows. Basic information for LGS 3 including our results is summarized in Table 10.

(1) *VRI* color-magnitude diagrams of \sim 490 stars in the 6:35 \times 6:35 area covering LGS 3 have been presented. These color-magnitude diagrams exhibit a well developed RGB, a small number of AGB stars, and several bright blue stars which are possibly young massive main-sequence stars.

(2) The tip of the RGB is found to be at $I=20.6 \pm 0.2$ mag and $(V - I)=1.31 \pm 0.05$ mag. From the I magnitude of the tip of the RGB, we derive a distance modulus of LGS 3 of $(m - M)_0=24.54 \pm 0.21$ mag, corresponding to a distance of 810 \pm 80 kpc.

(3) The mean color of the RGB at $M_I=-3.5$ mag is $(V - I)=1.28 \pm 0.05$ mag. From this value we obtain a mean metallicity of [Fe/H]=-2.10 \pm 0.22 dex.

(4) Surface photometry and star counts for LGS 3 have been presented. The surface brightness profiles combined with star number density profiles based on star counts are fitted by the single-mass isotropic King model with the core concentration parameter $c=1.25$ and the core radius $r_c=49'' \pm 3'' (=190 \pm 10$ pc). The central surface brightness of LGS 3 is measured to be $\mu_V(0)=24.81 \pm 0.07$ mag arcsec $^{-2}$.

The author is grateful to Mario Mateo for allowing the author to use his telescope time at Palomar, to Russ Day for his assistance at the telescope, and to Wendy Freedman and Leonard Searle for their support during the author's stay at the Carnegie Observatory. Sang Chul Kim is thanked for his help in obtaining the surface photometry of LGS 3. This research is supported in part by KOSEF Grant No. 941-0200-007-2 and by the Ministry of Education, Basic Science Research Institute Grant No. BSRI-94-5411.

REFERENCES

- Burstein, D., & Heiles, C. 1984, *ApJS*, 54, 33
 Caldwell, N., Armandroff, T. E., Seitzer, P., & Da Costa, G. S. 1992, *AJ*, 103, 840
 Carignan, C., Demers, S., & Côté, S. 1991, *ApJ*, 381, L13
 Christian, C. A., & Tully, R. B. 1983, *AJ*, 88, 934
 Christian, C. A., Adams, J. V., Butcher, H., Hayes, D. S., Mould, J. R., & Siegel, M. 1985, *PASP*, 97, 363
 Cook, K. H., & Olszewski, E. 1989, *BAAS*, 21, 775
 Da Costa, G. S., & Armandroff, T. E. 1990, *AJ*, 100, 162
 Davis, L. 1990, private communication
 Demers, S., & Irwin, M. 1993, *MNRAS*, 261, 657
 Demers, S., Irwin, M. J., & Kunkel, W. E. 1994, *AJ*, 108, 1648
 Djorgovski, S. 1988, in *Globular Cluster Systems in Galaxies*, IAU Symposium No. 126, edited by J. E. Harris and A. G. P. Philip (Kluwer, Dordrecht), p. 333
 Ferguson, H. C., & Binggeli, B. 1994, *A&AR*, 6, 67
 Gallagher III, J. S., & Wyse, R. F. G. 1994, *PASP*, 106, 1225
 Hargreaves, J. C., Gilmore, G., Irwin, M. J., & Carter, D. 1994, *MNRAS*, 269, 957
 Hunter, D. A., Hawley, W. M., & Gallagher III, J. S. 1993, *AJ*, 106, 1797
 I бата, R., Gilmore, G., & Irwin, M. 1994, *Nature*, 370, 194
 Irwin, M., & Hatzidimitriou, D. 1993, *The Globular Cluster-Galaxy Connection*, ASP Conf. Ser. Vol. 48, edited by G. H. Smith and J. P. Brodie, p. 322
 King, I. R. 1966, *AJ*, 71, 276
 Knapp, G., Kerr, F., & Bowers, P. 1978, *AJ*, 83, 360
 König, C. H. B., Nemeč, J. M., Mould, J. R., & Fahlman, G. G. 1993, *AJ*, 106, 1819
 Koribalski, B., Johnson, S., & Otrupcek, R. 1994, *MNRAS*, 270, L43
 Kowal, C. R., Lo, K. Y., & Sargent, W. L. W. 1978, *IAU Circ. No. 3305*
 Landolt, A. U. 1983, *AJ*, 88, 439
 Lee, M. G. 1990, Ph.D. thesis, University of Washington
 Lee, M. G. 1993, *ApJ*, 408, 409
 Lee, M. G. 1995, *AJ*, 110, 1155
 Lee, M. G., Freedman, W. L., & Madore, B. F. 1993a, *ApJ*, 417, 553
 Lee, M. G., Freedman, W. L., Mateo, M., Thompson, I., Roth, M., & Ruiz, M.-T. 1993b, *AJ*, 106, 1420
 Lo, K. Y., Sargent, W. L. W., & Young, K. 1993, *AJ*, 106, 507
 Mateo, M., Udalski, A., Szymanski, M., Kaluzny, J., Kubiak, M., & Krzeminski, W. 1994, preprint
 Mould, J. R., & Kristian, J. 1986, *ApJ*, 305, 591
 Mould, J. R., Bothun, G. D., Hall, P., Staveley-Smith, L., & Wright, A. E. 1990, *ApJ*, 362, L55
 Schechter, P., Mateo, M., & Saha, A. 1993, *PASP*, 105, 1342
 Schild, R. 1980, *ApJ*, 242, 63
 Schmidt, K.-H., & Boller, T. 1992, *ANac*, 313, 189
 Smecker-Hane, T. A., Stetson, P. B., Hesser, J. E., & Lehnert, M. D. 1994, *AJ*, 108, 507
 Tacconi, L. J., & Young, J. S. 1987, *ApJ*, 322, 681
 Thuan, T. X., & Martin, G. E. 1979, *ApJ*, 232, L11
 van de Rydt, F., Demers, S., & Kunkel, W. E. 1991, *AJ*, 102, 130
 Young, J. S., Xie, S., Kenney, J. D. P., & Rice, W. L. 1989, *ApJS*, 70, 699